

A HYBRID $L_2 - L_p$ VARIATIONAL MODEL FOR SINGLE LOW-LIGHT IMAGE ENHANCEMENT WITH BRIGHT CHANNEL PRIOR

Gang Fu, Lian Duan, Chunxia Xiao

Wuhan University, Wuhan, China
xyzgfu@gmail.com, lian.duan@whu.edu.cn, cxxiao@whu.edu.cn

ABSTRACT

In this paper, we consider and study the norm variable and propose a hybrid $L_2 - L_p$ variational model with bright channel prior based on Retinex to decompose an observed image into a reflectance layer and an illumination layer. Different from the existing methods, our proposed model can preserve the reflectance layer with more fine details while enforcing the illumination layer to be texture-less, avoiding the texture-copy problem. Moreover, for solving our non-linear optimization, we adopt an alternating minimization scheme to find the optimal. Finally, we test our algorithm on a large number of images and the experimental results illustrate that the proposed method has achieved the better result than other state-of-the-art methods both qualitatively and quantitatively.

Index Terms— Retinex, reflectance, illumination, alternating minimization

1. INTRODUCTION

According to Retinex theory [1], an image can be formulated by the product of a reflectance layer and an illumination layer. The reflectance layer depicts the intrinsic colors of the objects in the scene and the illumination layer represents the whole lighting in the scene. Many practical applications benefit from Retinex model, e.g. low-light image enhancement [2], intrinsic image decomposition [3], light information estimation [4].

It is an ill-posed problem to estimate the reflectance and illumination from a single image. Many methods have been proposed to handle this problem. Kimmel et al. [5] early proposed a variational framework for Retinex for single variable estimation. Wang et al. [6] proposed a total variational framework for Retinex. Fu et al. [7] proposed a weighted variational model for simultaneous reflectance and illumination estimation. Cai et al. [8] used a new joint intrinsic-extrinsic

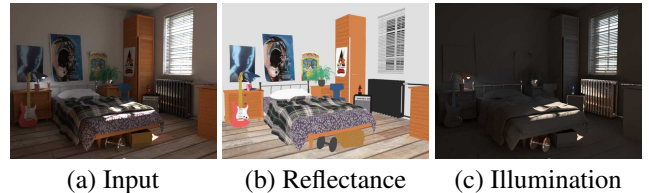


Fig. 1. The images are selected from the ARPR dataset [10].

prior for Retinex. Li et al. [9] further modeled noise component and constructed a unified framework to estimate reflectance, illumination and noise layers. These works rarely discuss the effects of norm for the estimation of reflectance and illumination. We in this paper consider and study the norm variable and propose a general framework with the L_p -norm ($0 \leq p \leq 2$).

According to Retinex theory [1], big gradients are more likely caused by the reflectance while small gradients are due to the illumination. Therefore, we argue that the illumination tends to be smoother than the reflectance in most regions. As shown in Fig. 1, the reflectance layer contains rich textures and details while the illumination is texture-less. Therefore, we use the L_2 -norm to constrain the reflectance with preserving more details and adopt the L_p ($0 \leq p \leq 2$) to constrain the illumination so as to avoid the texture-copy problem. We thus propose a hybrid $L_2 - L_p$ layer separation model to estimate both reflectance and illumination. Moreover, we analyze and discuss the effects of the norm variable on the reflectance and illumination layers. A visual illustration is shown in Fig. 2. Finally, we adopt an effective alternating minimization scheme to optimize our non-linear energy function. The experiment results show that our method has achieved better results than existing methods.

2. MODEL AND MODEL SOLVER

Based on the Retinex theory [1], an input image \mathbf{I} can be decomposed into a reflectance layer \mathbf{R} and an illumination layer \mathbf{S} , expressed as

$$\mathbf{I} = \mathbf{R} \cdot \mathbf{S}, \quad (1)$$

This work was partly supported by The National Key Research and Development Program of China (2017YFB1002600), the NSFC (No. 61672390), Wuhan Science and Technology Plan Project (No. 2017010201010109), and Key Technological Innovation Projects of Hubei Province (2018AAA062). Chunxia Xiao is the corresponding author.

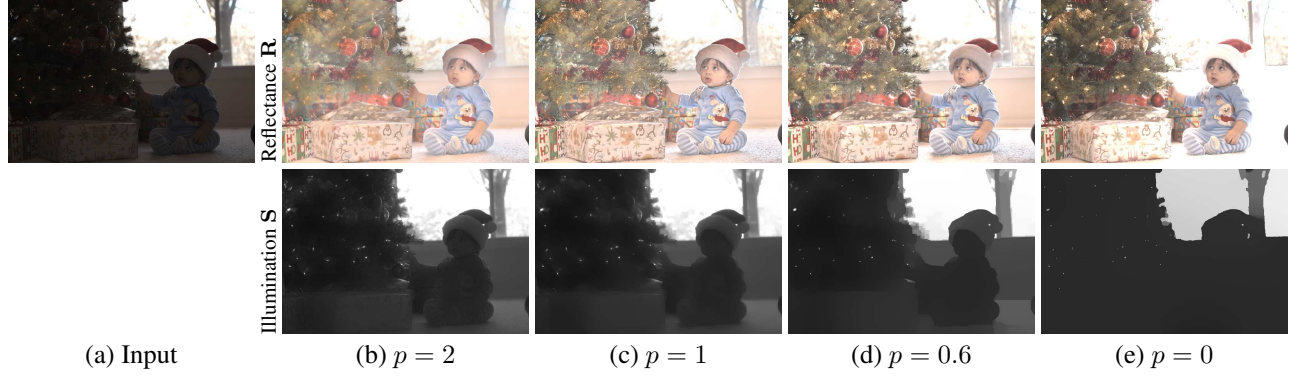


Fig. 2. Effect of norm variable p .

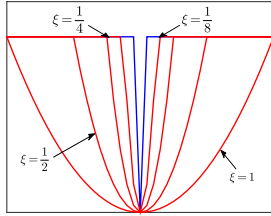


Figure 3. Plots of different penalty function. As can be seen, the penalty function $\Phi(\nabla s; \xi)$ (red curves) can approximate L_0 function (blue curve) well.

where \cdot denotes pixel-wise multiplication. Similar to existing methods, for simplicity, we assume that \mathbf{R} are RGB-vector and S is a scalar. In order to the speed and validity of calculation, we compute in HSV channels, as done in [7, 11, 8]. From Eqn. (1), we have the single-channel image model, expressed as

$$I = R \cdot S. \quad (2)$$

Taking a logarithm operation on both side of the above Eqn. (2), yields

$$i = r + s, \quad (3)$$

where $i = \log I$, $r = \log R$, $s = \log S$.

Let us think back to the assumption of the Retinex theory. It says that the reflectance tends to be piece-wise constant and the illumination is locally smooth. Many methods [6, 12, 7, 5] based on the Retinex theory have been proposed, based on this assumption. They usually regularize the reflectance using the L_1 -norm and the illumination using the L_2 -norm. In contrast, we adopt the L_2 -norm to constraint the reflectance to as far as possible preserve tiny details and the L_p -norm to constraint the illumination to avoid the texture-copy problem. Therefore, we formulate layer decomposition as an energy minimization problem as

$$\min_{r,s} ||i - r - s||^2 + \lambda_r ||\nabla r||^2 + \lambda_s ||\nabla s||^p + \lambda_b ||\nabla s - s_0||^2, \quad (4)$$

where λ_r, λ_s are the balancing weights for regularizing the reflectance and illumination layers, respectively, ∇ is the gradient operator including horizontal and vertical directions and $||\cdot||^p$ denotes p norm ($0 \leq p \leq 2$). Note that the L_0 -norm

($p = 0$) can result in smoother result, e.g., [13, 14, 15]. We set p to 0.4 in default, and find that it basically meet our demand for texture filtering. The first term $||i - r - s||^2$ is a data term measuring the error between the reconstruct image and the input image. The second term $||\nabla r||^2$ is an L_2 -norm term for regularizing the reflectance, the third term $||\nabla s||^p$ term is a p -norm term for regularizing the illumination, and the fourth term $||\nabla s - s_0||^2$ is our bright channel prior term. The constant variable s_0 is defined as $s_0 = \log S_0$, where S_0 is our bright channel intensity of the observed image \mathbf{I} . Similar to [16, 8, 17], S_0 can be written as $S_0 = 1 - \min_{\Omega} (\min_{c \in \{r,g,b\}} (1 - \mathbf{I})^c) = \max_{\Omega} (\max_{c \in \{r,g,b\}} \mathbf{I}^c)$, where Ω is a small patch, e.g., a 4×4 window. This bright channel prior provides some useful cues for layer separation [11], avoiding the ambiguity in decomposition to some extent.

Optimization. As in [8], we adopt a block coordinate descent algorithm [18] to find the optimal solution to the non-convex energy minimization (4). Since the L_p -norm in the regularization term on illumination leads non-smooth optimization, we use an iteratively re-weighted least square method [19] and rewrite the regularization term on illumination as $||\nabla s||^p = u ||\nabla s||^2$, where $u = (\nabla s + \epsilon)^{p-2}$ when $0 < p \leq 2$, and

$$u = \begin{cases} \frac{1}{\xi^2}, & \text{if } |\nabla s| < \xi \\ \frac{1}{||\nabla s||^2}, & \text{otherwise} \end{cases}, \quad (5)$$

when $p = 0$. We here set to $\xi = \frac{1}{8}$. Note that the variable u is only approximate, since we use a 2-norm format $\Phi(\nabla s; \xi)$ in [14] to approximate the L_0 -norm function, as shown in Fig. 3. Please refer to [14] for more details about this approximation operation.

Note that we consider the variable u as known in each iteration calculation. Therefore, two separated sub-problem are iteratively solved. In particular, for the k th iteration, we have

$$(P1) \min_{s^k} ||i - r^{k-1} - s||^2 + \lambda_s u ||\nabla s||^2 + \lambda_b ||s - s_0||^2,$$

$$(P2) \min_{r^k} ||i - r - s^k||^2 + \lambda_r ||\nabla r||^2.$$

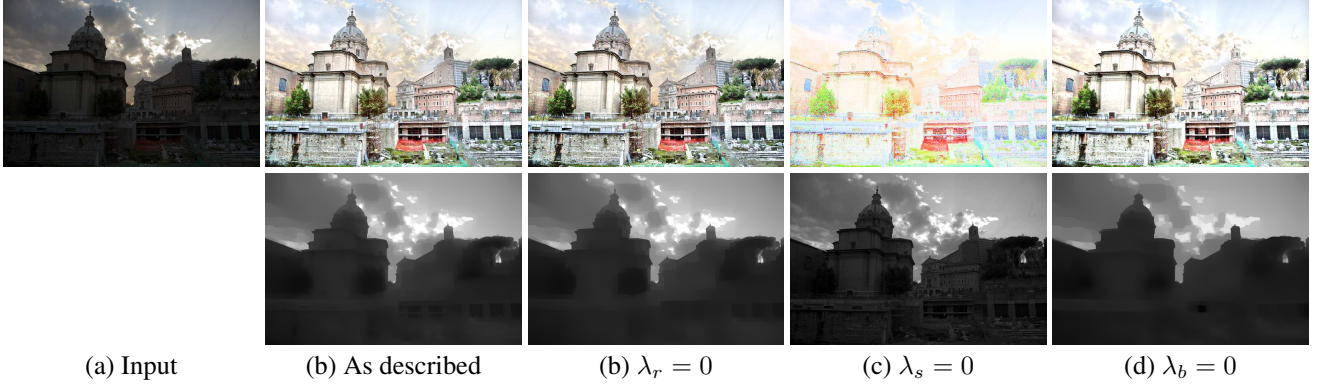


Fig. 4. Algorithm variants. To show the effect of each constraint, we remove different regularization terms.

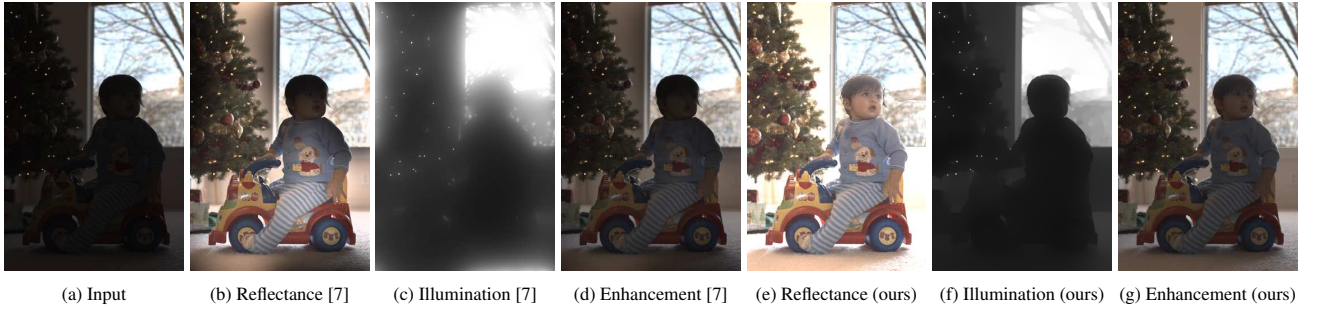


Fig. 5. Comparison with the state-of-the-art method (WVM) [7], including: Retinex composition and enhancement.

We can see that the energy minimization problem now only includes quadratic terms and thus have closed-form optimal solutions. We will give the detailed algorithm in the following.

(i) *Algorithm for (P1)*: The energy can be rewritten in the matrix form as: $(\tilde{s} - s)^T(\tilde{s} - s) + \lambda_s(s^T \mathbf{D}_x^T \mathbf{U}_x \mathbf{D}_x s + s^T \mathbf{D}_y^T \mathbf{U}_y \mathbf{D}_y s) + \lambda_b(s - s_0)^T(s - s_0)$, where $\tilde{s} = \mathbf{i} - \mathbf{r}^{k-1}$. Here \mathbf{D}_x and \mathbf{D}_y are the Toeplitz matrices from the discrete gradient operators with forward difference. \mathbf{U}_x and \mathbf{U}_y represent diagonal matrices containing the weights u_x and u_y . The variable s can be uniquely estimated by the solution of a linear system as $s_k = (\lambda_s \mathbf{L}^k + (\lambda_b + 1) \mathbb{I})^{-1}(\tilde{s} + \lambda_b s_0)$, where \mathbb{I} is an identity matrix, and $\mathbf{L}^k = \mathbf{D}_x^T \mathbf{U}_x \mathbf{D}_x + \mathbf{D}_y^T \mathbf{U}_y \mathbf{D}_y$ is a five-point positive definite Laplacian matrix [20].

(ii) *Algorithm for (P2)*: Similar to the optimization of (P1), we can update r^k by $r^k = (\mathbb{I} + \lambda_s \mathbf{M}^k)^{-1} \tilde{r}$, where $\mathbf{M} = \mathbf{D}_x^T \mathbf{D}_x + \mathbf{D}_y^T \mathbf{D}_y$, $\tilde{r} = \mathbf{i} - s^k$.

The variables s, r are iteratively estimated until $\epsilon_s = \|\mathbf{s}^k - \mathbf{s}^{k-1}\| / \|\mathbf{s}^{k-1}\| \leq \epsilon$ and $\epsilon_r = \|\mathbf{r}^k - \mathbf{r}^{k-1}\| / \|\mathbf{r}^{k-1}\| \leq \epsilon$, or the maximum number of iterations to reach a given constant K . In our experimental results, we can obtain stable and ideal results through 20 iterations (see Fig. 7). Once obtaining the variables r and s , we can estimate the single-channel reflectance layer $R = e^r$ and illumination layer $S = e^s$. With obtaining the results in HSV space, we can convert them to RGB space and then obtain color reflectance layer.

3. RESULTS

We perform our Matlab implementation on a PC with Manjaro system, Intel Core i7 CPU, 16GB RAM. In our experiment, we set $\lambda_r = 0.001$, $\lambda_s = 0.01$, $\lambda_b = 0.15$, $\epsilon = 0.001$.

Retinex decomposition. The visual comparison results are shown in Fig 5. Here we mainly compare our method with the weighted variation model (WVM) proposed by Fu et al. [7]. Our estimated illumination is more texture-less and can preserve the structure of scene well, due to the L_p -norm. In other words, our model can effectively avoid that high-frequency textures belonged to the reflectance layer wrongly are assigned to the illumination layer. The illumination layer of WVM [7] may break the structure of the scene and over-smoothed, although it can filter many textures.

Effect of the norm p . As shown in Fig. 2, with the reduction of p , we can see that the illumination is getting smoother and more texture-less. We also notice that when $p = 0$, the illumination layer may lose some structure information, since the L_0 -norm have stronger sparsity than other norm format [13], e.g., the common edge-aware L_1 -norm.

Illumination adjustment. For a given low-light image, we can adjust its illumination layer to generate visually clear results. Here, the Gamma correction is adopted for adjusting it, mathematically expressed as $S' = S^{1/\gamma}$ (empirically set γ to 2.2). The final enhanced image I' is obtained by $I' =$

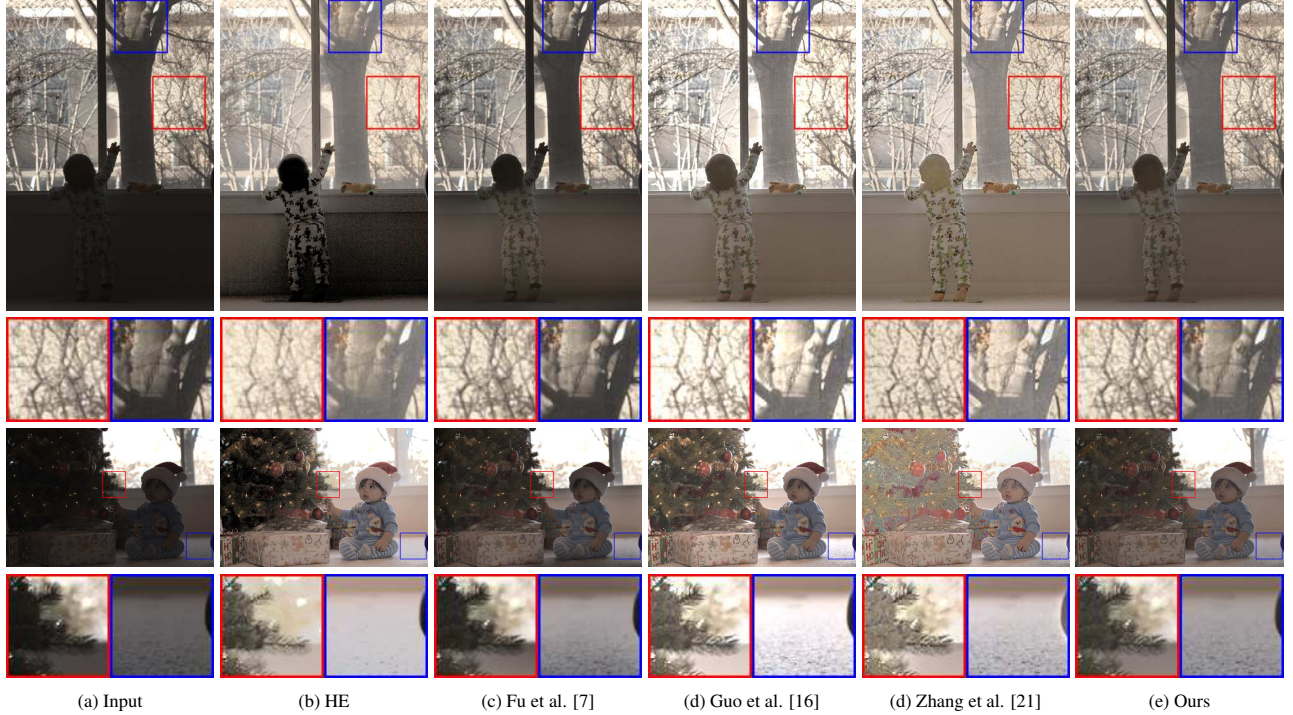


Fig. 6. Comparison with other state-of-the-art methods for low-light image enhancement.

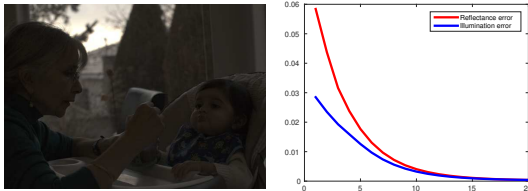


Fig. 7. Convergence curve of our algorithm. **Left:** the input image. **Right:** the x - and y -coordinate refer to the iteration number and ϵ_s (ϵ_r), respectively.

$R \cdot S'$. Note that the Gamma correction is performed in the HSV domain to preserve color information better.

We compare our proposed method with other existing methods, including histogram equalization (HE) method, and the methods of [7], [16], [21]. Some visual comparison examples are shown in Fig. 6. There are often unnatural regions in the results estimated by HE method, e.g. the area where the child's feet near the window are. The results estimated by [7] sometimes are under-enhanced, e.g., Christmas tree with green leaves. In addition, the methods of [16, 21] sometimes over enhance some regions, e.g., green leaves on the Christmas. In contrast, our method produces natural-looking results.

Quantitative evaluation. Since the ground truth of the enhanced image is almost impossible to get, we adopt natural image quality evaluator (NIQE) [22] and autoregressive-

Table 1. Quantitative comparison with NIQE and ARSIM.

Algorithms	NIQE	ARSIM
HE	3.120	2.892
Fu et al. 2016 [7]	2.870	2.224
Guo et al. 2017 [16]	2.631	2.314
Zhang et al. 2018 [21]	2.240	2.302
Ours	2.012	2.114

based image sharpness metric (ARSIM) [23] to evaluate the performance, as in [8, 7, 11]. The lower NIQE/ARSIM value denotes the higher enhanced image quality. We choose the HDR dataset [24] to quantitatively compare our method with other methods. As shown in Table 1, our algorithm achieves a lower average on NIQE/ARSIM than other state-of-the-art algorithms. This is due to that our hybrid $L_2 - L_p$ model can reasonably enhance the low-light regions and not overexpose some bright regions, leading to more natural results.

4. CONCLUSION

We have designed a hybrid $L_2 - L_p$ layer separation model to simultaneously estimate the reflectance and illumination layers. Moreover, an alternation optimization scheme is adopted to effectively optimize our non-linear energy function. We employ the HDR dataset and perform various experiments to evaluate our model. The experiments show that our method has achieved better results than other methods.

5. REFERENCES

- [1] E. H. Land and J. J. McCann, "Lightness and retinex theory," *Journal of the Optical Society of America*, vol. 61, no. 1, pp. 1–11, 1971.
- [2] L. Li, R. Wang, W. Wang, and W. Gao, "A low-light image enhancement method for both denoising and contrast enlarging," in *ICIP*, 2015, pp. 3730–3734.
- [3] Q. Zhao, P. Tan, Q. Dai, L. Shen, E. Wu, and S. Lin, "A closed-form solution to retinex with nonlocal texture constraints," *IEEE Transactions on Pattern Analysis and Machine Intelligence*, vol. 34, no. 7, pp. 1437–1444, 2012.
- [4] L. Zhang, Q. Yan, Z. Liu, H. Zou, and C. Xiao, "Illumination decomposition for photograph with multiple light sources," *IEEE Transactions on Image Processing*, vol. 26, no. 9, pp. 4114–4127, 2017.
- [5] R. Kimmel, M. Elad, D. Shaked, R. Keshet, and I. Sobel, "A variational framework for retinex," *International Journal of Computer Vision*, vol. 52, no. 1, pp. 7–23, 2003.
- [6] M. K. Ng and W. Wang, "A total variation model for retinex," *Imaging Sciences*, vol. 4, no. 1, pp. 345–365, 2011.
- [7] X. Fu, D. Zeng, Y. Huang, X. Zhang, and X. Ding, "A weighted variational model for simultaneous reflectance and illumination estimation," in *CVPR*, 2016.
- [8] B. Cai, X. Xu, K. Guo, K. Jia, B. Hu, and D. Tao, "A joint intrinsic-extrinsic prior model for retinex," in *ICCV*, 2017.
- [9] M. Li, J. Liu, W. Yang, X. Sun, and Z. Guo, "Structure-revealing low-light image enhancement via robust retinex model," *IEEE Transactions on Image Processing*, vol. 27, no. 6, pp. 2828–2841, 2018.
- [10] N. Bonneel, B. Kovacs, S. Paris, and K. Bala, "Intrinsic decompositions for image editing," *Computer Graphics Forum*, vol. 36, no. 2, 2017.
- [11] X. Fu, Y. Liao, D. Zeng, Y. Huang, X. Zhang, and X. Ding, "A probabilistic method for image enhancement with simultaneous illumination and reflectance estimation," *IEEE Transactions on Image Processing*, vol. 24, no. 12, pp. 4965–4977.
- [12] Y. Zang, Z. Pan, J. Duan, G. Wang, and W. Wei, "A double total variation regularized model of retinex theory based on nonlocal differential operators," in *International Congress on Image and Signal Processing*, 2013.
- [13] L. Xu, C. Lu, Y. Xu, and J. Jia, "Image smoothing via l_0 gradient minimization," *ACM Transactions on Graphics*, vol. 30, no. 6, pp. 174:1–174:12, 2011.
- [14] L. Xu, S. Zheng, and J. Jia, "Unnatural l_0 sparse representation for natural image deblurring," in *CVPR*, 2013.
- [15] Liang Z., Xu J., Zhang D., Cao Z., and Zhang L., "A hybrid l_1 - l_0 layer decomposition model for tone mapping," in *CVPR*, 2018.
- [16] X. Guo, Y. Li, and H. Ling, "Lime: Low-light image enhancement via illumination map estimation," *IEEE Transactions on Image Processing*, vol. 26, no. 2, pp. 982–993, 2017.
- [17] X. Fu, D. Zeng, Y. Huang, X. Ding, and X. P. Zhang, "A variational framework for single low light image enhancement using bright channel prior," in *IEEE Global Conference on Signal and Information Processing*, 2013.
- [18] P. Tseng, "Convergence of a block coordinate descent method for nondifferentiable minimization," *Journal of optimization theory and applications*, vol. 109, no. 3, pp. 475–494, 2001.
- [19] E. J. Candes, M. B. Wakin, and S. P. Boyd, "Enhancing sparsity by reweighted l_1 minimization," *Journal of Fourier analysis and applications*, vol. 14, no. 5-6, pp. 877–905, 2008.
- [20] D. Krishnan, R. Fattal, and R. Szeliski, "Efficient preconditioning of laplacian matrices for computer graphics," *ACM Transactions on Graphics*, vol. 32, no. 4, pp. 142:1–142:15, 2013.
- [21] Q. Zhang, G. Yuan, C. Xiao, L. Zhu, and W. Zheng, "High-quality exposure correction of underexposed photos," in *ACM International Conference on Multimedia*, 2018.
- [22] A. Mittal, R. Soundararajan, and A. C. Bovik, "Making a "completely blind" image quality analyzer," *IEEE Signal Processing Letters*, vol. 20, no. 3, pp. 209–212, 2013.
- [23] K. Gu, G. Zhai, W. Lin, X. Yang, and W. Zhang, "No-reference image sharpness assessment in autoregressive parameter space," *IEEE Transactions on Image Processing*, vol. 24, no. 10, pp. 3218–3231, 2015.
- [24] P. Sen, N. Khademi Kalantari, M. Yaesoubi, S. Darabi, D. B. Goldman, and E. Shechtman, "Robust patch-based hdr reconstruction of dynamic scenes," *ACM Transactions on Graphics*, vol. 31, no. 6, pp. 203:1–203:11, 2012.